Improved $BaBi_4Ti_4O_{15}$ Relaxor Ferroelectrics for FRAM Application

A Thesis Submitted in Partial Fulfillment of the
Requirements for the Degree of

Bachelor of Technology

by

Ramendra Sundar Subudhi

(Roll No. 10608017)

Supervisor:

Dr. JAPES BERA

Department of Ceramic Engineering.

National Institute of Technology, Rourkela, Odisha.

ACKNOWLEDGEMENTS

With deep regards and profound respect, I avail this opportunity to express my deep sense of gratitude and indebtedness to Prof. Japes Bera, Head of the Department, Department of Ceramic Engineering, N. I. T. Rourkela, for introducing the present research topic and for inspiring guidance, constructive criticism and valuable suggestion throughout this research work. It would have not been possible for me to bring out this project report without his help and constant encouragement. I wish that he will keep in touch with me in future and will continue to give his valuable advice.

I would like to express my gratitude, to my faculty adviser Prof. Santanu Bhattacharyya, for his cooperation in one way or the other. I wish to record my thanks and gratitude to him for his valuable suggestions and encouragements at various stages of the work .I am also grateful to all the faculties of Department of Ceramic Engineering, whose vast knowledge in the field of science and technology has enlightened me in different areas of this experimental research work.

I am also thankful to Miss. Arundhati Chakrabarti and other research scholars in Department of Ceramic Engineering for providing all joyful environment in the lab and helping me.It was a nice and memorable association with all the stuff of my department. I wish to give them my heartfelt thanks for their constant help.

I would also like to thank my papa for constantly encouraging me to give my 100 % and work hard till I achieve my goal.

Above all, I thank our savior GOD for giving me all these people to help and encourage me, and for the skills and opportunity to complete this report.

Date: (Ramendra Sundar Subudhi)

National Institute of Technology
Rourkela

CERTIFICATE

This is to certify that the thesis entitled, *"Improved $BaBi_4Ti_4O_{15}$ Relaxor Ferroelectrics for FRAM Application"* submitted by Mr. **Ramendra Sundar Subudhi** in partial fulfillments for the requirements for the award of **Bachelor of Technology** degree in **Ceramic Engineering** at National Institute of Technology, Rourkela is an authentic work carried out by her under my supervision and guidance.

To the best of my knowledge, the matter embodied in the thesis has not been submitted to any other University/ Institute for the award of any Degree or Diploma.

Date:

Dr. Japes Bera

(Head of the Department)

Dept. of Ceramic Engineering

National Institute of Technology

Rourkela-769008

CONTENTS

List of Tables

List of Figures

Fig.11. Plot of ferroelectric hysteresis loop measured at room temperature for different $Ba_{1-x}Na_xBi_4Ti_{4-x}Nb_xO_{15}$ (x = 0.2, 0.4, 0.6) ceramics.

Fig.12. Plot of $2P_r$ and $2E_c$ measured at room temperature for different $Ba_{1-x}Na_xBi_4Ti_{4-x}Nb_xO_{15}$ (x = 0.2, 0.4, 0.6) ceramics.

Fig.13. Cole-Cole plot for $Ba_{1-x}Na_xBi_4Ti_{4-x}Nb_xO_{15}$ (x = 0.2, 0.4, 0.6) ceramics at 600^oC.

Chapter 1

Abstract

1. Abstract:

Bi-based Aurivillius family of compounds have received considerable attention as the materials for ferroelectric random access memory (FRAM) because of their low operating voltage, fast switching speed, large remnant polarization, low coercive field, superior polarization fatigue resistant characteristics and high Curie temperature. A large remnant polarization, low coercive field and high Curie temperature are required for better performance of FRAM devices. Majority of Aurivillius oxides are normal ferroelectrics, while only a few of them such as $BaBi_2Nb_2O_9$, $BaBi_2Ta_2O_9$, $BaBi_4Ti_4O_{15}$ etc. exhibit relaxor behaviour. Relaxor ferroelectrics are attractive for a wide range of applications owing to their excellent high dielectric and piezoelectric responses over a wide range of temperatures. Ferroelectric properties of these compounds are often improved by chemical lattice site engineering. This is done by suitable atomic substitutions at 'A' and/or 'B' of the structure. Nb^{5+} substitution at 'B' site has been proved to be an most effective site engineering in 2 and 3 layered compounds. In the present study, Nb^{5+} has been substituted at 'B'-site and Na^{1+} at 'A'-site to compensate charge in the formulation $Ba_{1-x}Na_xBi_4Ti_{4-x}Nb_xO_{15}$. Effect of the substitution on the structural, microstructural, dielectric and ferroelectric properties were evaluated. The AC complex impedance spectroscopy was used to analyze the change in dielectric conductivity of the ceramics. An improved permittivity, increased remnant polarization and decreased coercive field were found in the Nb-substituted compound.

Chapter 2

Introduction

2. Introduction:

Ferroelectric RAM (FeRAM or FRAM) is a random access memory similar in construction to DRAM but uses a ferroelectric layer instead of a dielectric layer to achieve non-volatility. FRAM is one of a growing number of alternative non-volatile memory technologies that offer the same functionality as Flash memory. FRAM advantages over flash include lower power usage, low leakage currents, faster write performance and a much greater maximum number (exceeding 10^{16} for 3.3 V devices) of write-erase cycles.

Bi-based Aurivillius family of compounds has received considerable attention as the materials for ferroelectric random access memory (FRAM) because of their low operating voltage. They have very fast switching speed. It has large remnant polarization and low coercive field. They have superior polarization fatigue resistant characteristics and high Curie temperature [1-7]. For better performance of FRAM devices a large remnant polarization is required. FRAM requires low coercive field for good performance. High Curie temperature is required for best performance of FRAM devices.

Majority of Aurivillius oxides are normal ferroelectrics, while only a few of them such as $BaBi_2Nb_2O_9$, $BaBi_2Ta_2O_9$, $BaBi_4Ti_4O_{15}$ etc. exhibit relaxor behaviour [3, 8, 9]. Relaxor ferroelectrics are attractive for a wide range of applications owing to their excellent high dielectric and piezoelectric responses over a wide range of temperatures [10, 11].

Bi-layered structure Aurivillius compound is generalized as $Bi_2A_{m-1}B_mO_{3m+3}$. The structure consists of 'm' number of $(A_{m-1}B_mO_{3m+1})^{2-}$ slabs sandwiched between $(Bi_2O_2)^{2+}$ layers, where '*A*' represents monovalent, divalent or trivalent element and '*B*' represents tetravalent, pentavalent or hexavalent metallic cations which are in 12-fold and 6-fold co-ordination respectively [4, 10, 11]. $BaBi_4Ti_4O_{15}$ (BBT) is a four layered ('*m*'=4) compound with structural formula $[(Bi_2O_2)^{2+}((BaBi_2)Ti_4O_{13})^{2-}]$, where the Ba- and Bi-ions occupies the *A*-site and Ti-ions resides in the *B*-site. Their intrinsic electrical properties are anisotropic, with the maximum value of conductivity and the major component of spontaneous polarization parallel to the $(Bi_2O_2)^{2+}$ layers. As a result, properties of the polycrystalline

materials are strongly affected by their microstructure, especially by the orientation of the plate-like grains and by the length-to-thickness ratio (aspect ratio) of the grains [12, 13].

Ferroelectric properties of these compounds are often improved by chemical lattice site engineering. This is done by suitable atomic substitutions at '*A*' and/or '*B*' of the structure. Nb^{5+} substitution at '*B*' site has been proved to be most effective site engineering in 2 and 3 layered compounds.

Chapter 3

Literature Review

3. Literature Review:

3.1. General Introduction:

The family of bismuth oxides was discovered more than 50 years ago by Aurivillius [14]. Recently, interest in the properties of the Aurivillius phases as temperature-stable ferro-piezoelectrics has been renewed. Several bismuth-layered crystal structures and their properties have been investigated in detail. The majority of those materials are normal ferroelectrics with a fairly high Curie temperature, while only a few of them such as $BaBi_2Nb_2O_9$, $BaBi_2Ta_2O_9$, etc. exhibit relaxor behavior [15-17]. Relaxor materials are characterized by frequency dispersion having broad dielectric normally near the dielectric maximum. The latter properties are very useful for a wide range of applications due to their extremely high dielectric and piezoelectric responses in a wide range of temperatures [18]. The Bi-based Aurivillius family of oxides has proved to be a promising candidate for the growing need of new lead-free materials for various applications. BBT is a member of this large family of compounds and is a promising candidate for high-temperature piezoelectric applications, memory application and ferroelectric non volatile memories (Fe-RAM) but a lot of aspects of the preparation and properties of BBT remain unexplored.

The lattice structure of the Aurivillius family of compounds is composed of *m* number of like perovskite $(A_{m-1}B_mO_{3m+3})^{2-}$ unit cells sandwiched between $(Bi_2O_2)^{2+}$ slabs along pseudo tetragonal c-axis (*m* is an integer between 1 and 5). The 12 coordinate perovskite like *A*-site is typically occupied by a large cation such as Na^+, K^+,Ca^{2+}, Sr^{2+}, Ba^{2+}, Pb^{2+}, Bi^{3+} or Ln^{3+} and the 6-coordinate perovskite like *B*-site by smaller cations such as Fe^{3+}, Cr^{3+}, Ti^{4+}, Nb^{5+} or W^{6+}. BBT, as the *m* = 4 member of the Aurivillius family has Ba and Bi ions at the *A*-sites and Ti ions at the *B*-sites of the perovskite block $[(Bi_2O_2)^{2+}\cdot((BaBi_2)Ti_4O_{13})^{2-}]$ [15].

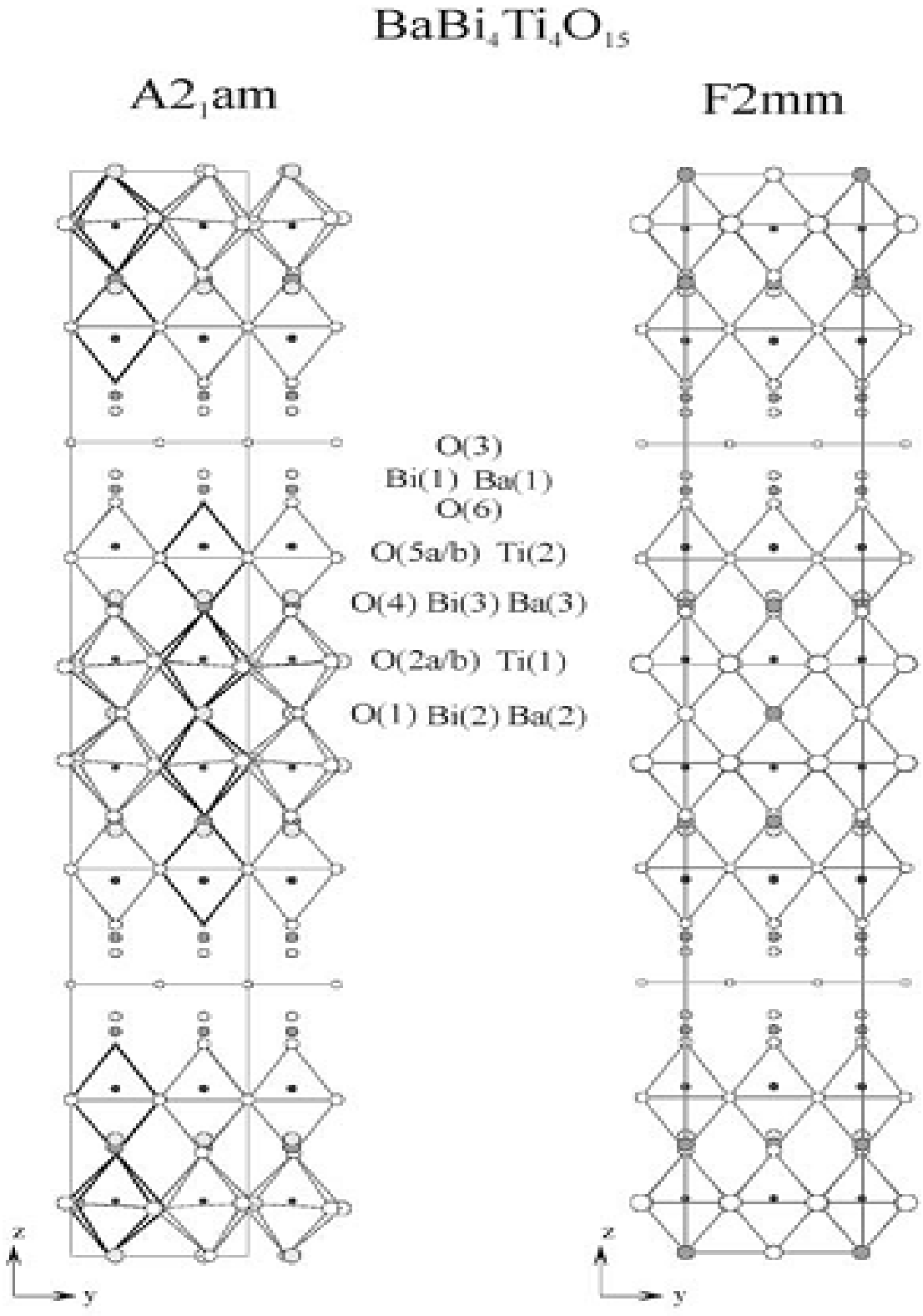

Fig.1. Crystal structures of $BaBi_4Ti_4O_{15}$

3.2. Requirement of doping:

The disadvantage of the layer-structure perovskite materials for high-temperature piezoelectric applications is their relatively high conductivity. This conductivity is electronic *p*-type, therefore, can be suppressed by donor doping [19–22]. The *p*-type conductivity observed in layer-structure perovskite materials is related to the creation of electron holes that result from the compensation of intrinsic structural defects (cation vacancies) or acceptor impurities. The dominant structural defects producing electron holes in BBT are not known. The concentration of electron holes and, consequently, the material's conductivity are increased by acceptor doping and decreased by donor doping [19–22]. However, the effect of aliovalent dopants is relatively small. For example, the minimum conductivity in air sintered $BaBi_4Ti_4O_{15}$ ceramics was obtained by the substitution of 5 mol % of the Ti^{4+} ions with Nb^{5+} donors, and this resulted in a conductivity decrease of 2 orders of magnitude [22].

3.3. Effect of dopants:

Niobium doping decreases the grain size and suppresses the grain growth in BBT ceramics [23]. Nb^{5+}donors incorporate into the BBT structure at the Ti^{4+}sites cause an increase in the barium concentration and decrease the bismuth concentration. Excess donor charge is mainly compensated by a decrease in the average valency of the A sites in the perovskite $(A_3B_4O_{13})^{2-}$ block of the $(Bi_2O_2)^{2-}$. $((BaBi_2)Ti_4O_{13})^{2+}$) layered structure with the incorporation of more 2-valent barium ions and fewer 3-valent bismuth ions.

Doping of BBT with Nb changes the temperature of the dielectric constant maximum (Curie temperature, T_C), strongly suggesting incorporation of the dopants into the $BaBi_4Ti_4O_{15}$ structure. Substitution of the Ti ions in the $BaBi_4Ti_4O_{15}$ structure by Nb ions decreases the Curie temperature (T_C) by approximately 7 $^oC/mol\%\ Nb_{Ti}$. Nb increases the room-temperature dielectric constant of $BaBi_4Ti_4O_{15}$ceramics. The Nb doping changes the shape of the dielectric-constant maximum. Whereas the low Nb concentrations, up to 2

mol%, increase the dielectric constant at T_C, the higher Nb concentrations suppressed the dielectric-constant maximum. Broadening of the dielectric-constant maximum can be related to the changes in the microstructure with Nb doping, e.g. the appearance of secondary phases, the non-homogeneous distribution of dopants and/or the decrease in grain size [23].

Compensatory doping of sodium in place of 12-fold co-ordinated Ba greatly affects the properties.The T_C temperature decreases as a consequence of the substitution of larger 12-fold coordination Ba^{2+} cations for smaller cations such as Na^{+}. For high Na contents, the microstructure is dominated by the presence of large rounded edges platelet-like grains. This grain shape is observed for many bismuth layered materials and is connected with the strong anisotropy of the crystal structure. The rounded edges are characteristic of liquid phase sintering. Curie temperature as well as the temperature of the maximum permittivity decrease regularly as the sodium concentration decreases. The decrease of the Curie temperature with increasing size of the 12-coordinated cations in the Aurivillius compounds has been attributed to the increase of the tolerance factor which leads to a less distorted structure [24].

3.4. Synthesis:

The properties of ceramics are greatly affected by the characteristics of the powder, such as particle size, morphology, purity and chemical composition. Various chemical methods, e.g.co-precipitation, sol–gel, hydrothermal and colloid emulsion techniques are used to efficiently control the morphology and chemical composition of prepared powder. The citrate gel process offers a number of advantages for the preparation of fine powders of many complex oxides as quoted in the literature [8–11].The main drawback of this process is the possible formation of carbonate during decomposition of the polymeric gel.

Non-Conventional methods are used to get better homogeneous and reactive precursor powder compared to solid-state method. Usually Ti-alkoxides and Ti-chlorides are used as the Ti-metal source in chemical routes. Since Ti-alkoxides/nitrates are relatively costlier and solid state route is less time consuming and cheaper method so solid state route was selected.

3.5. Summary of literature:

From the literature review it was found that there is no report of Nb^{+5} substitutions in $BaBi_4Ti_4O_{15}$ relaxor ferroelectrics.Niobium doping suppresses the grain growth in $BaBi_4Ti_4O_{15}$ ceramics. Doping of $BaBi_4Ti_4O_{15}$ with Nb changes the temperature of the dielectric constant maximum (Curie temperature,T_C) ,strongly suggesting incorporation of the dopants into the $BaBi_4Ti_4O_{15}$ structure. Substitution of the Ti ions in the $BaBi_4Ti_4O_{15}$ structure by Nb ions decreases the Curie temperature (T_C). Nb substitution increases the room-temperature dielectric constant of $BaBi_4Ti_4O_{15}$ceramics. The T_C temperature decreases as a consequence of the substitution of larger 12-fold coordination Ba^{2+} cations for smaller cations such as Na^{+}.

3.6. Objective of work:

- A & B site substitution to improve the relaxor ferroelectric property
    - ✓ Nb^{5+} substitution for Ti^{4+} because Nb^{5+} has been reported to enhance the relaxor property.
    - ✓ Na^{1+} substitution for Ba^{2+} to compensate Nb^{5+} substitution in the structure.Na^{1+} ahs also been reported as a useful substituent in aurivillus compound.

Chapter 4

Experimental Procedure

4. Experimental

4.1. Experimental procedure:

Polycrystalline samples of $Ba_{1-x}Na_xBi_4Ti_{4-x}Nb_xO_{15}$ (BTN*X*) with x = 0.2, 0.4, 0.6 compositions (abbreviated as BTN2, BTN4, BTN6 respectively) were prepared by solid state reaction. Stoichiometric amounts of $BaCO_3$, Bi_2O_3, TiO_2, Na_2CO_3 and Nb_2O_5 were mixed in an agate mortar using isopropyl alcohol as the liquid media. The mixed powders were calcined at 800, 900, 1000 and 1050^oC depending on the composition with intermittent grinding after each heating step. Phase identification of calcined powders was performed using a Cu Kα X-ray Diffractometer (PW-1830, Philips, Netherlands). The final BTNX powders were pelletized at a pressure of 220 MPa using poly vinyl alcohol as a binder. The pellets were sintered at 1100^oC and the soaking period varied from 1 to 6 h depending on the composition. The density of sintered pellets was determined by Archimedes' method. The microstructures of sintered specimens were studied using Scanning electron microscopy (JSM-6480LV). For dielectric measurement, sintered pellets were electroded with silver conductive electrode paste (Alfa Aesar) to provide the ohmic contacts. The dielectric properties and complex impedance were measured using an Impedance Analyzer (Solatron 1260). All the dielectric data were collected while heating at a rate of 1^oC/min. A standard ferroelectric analyzer (PE loop tracer, Marine India Electronics) was used to trace *P-E* hysteresis loops.

4.2. Flow chart for preparation of BTNX:

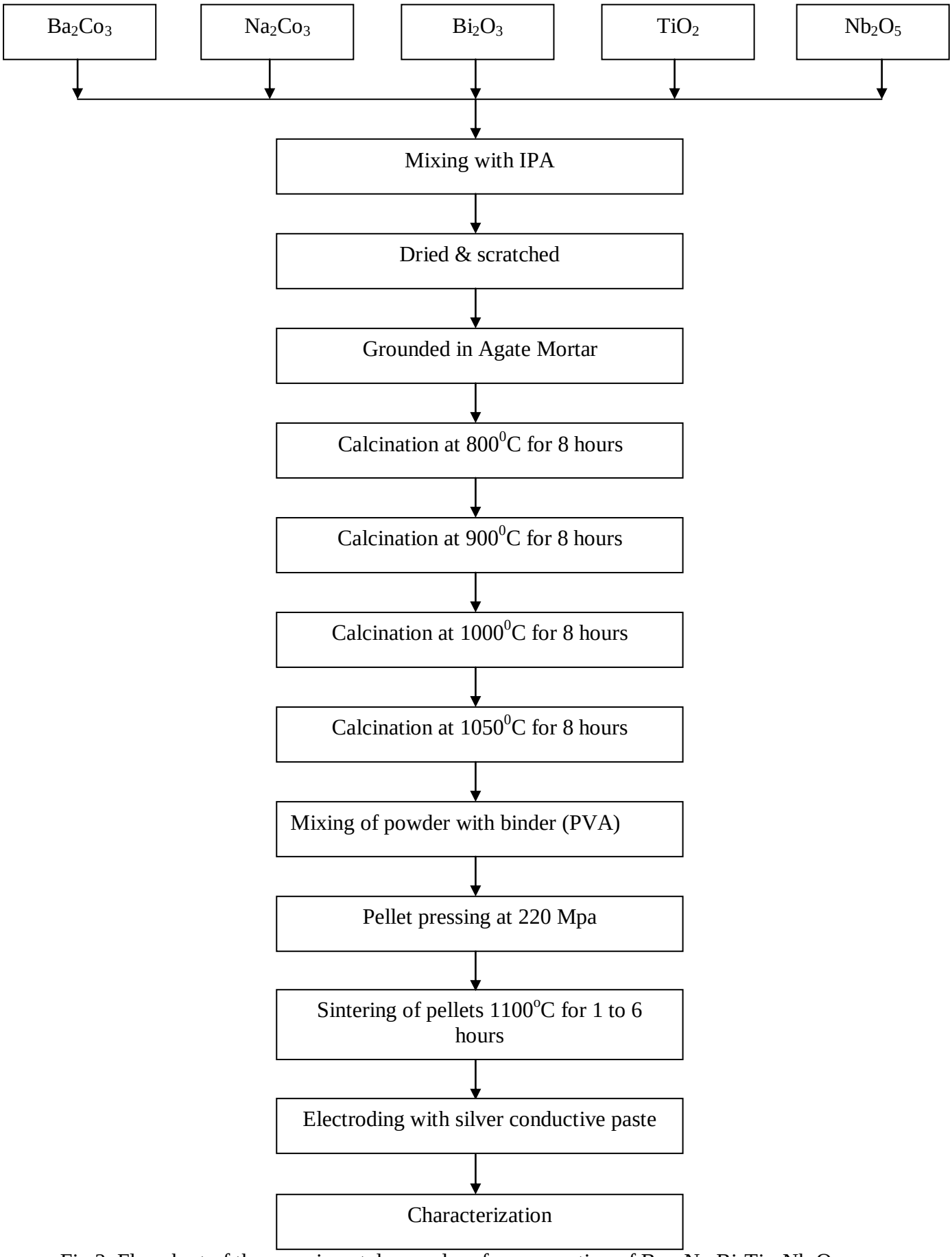

Fig.2. Flowchart of the experimental procedure for preparation of $Ba_{1-x}Na_xBi_4Ti_{4-x}Nb_xO_{15}$

Chapter 5

Results and discussion

5. Results and discussion

5.1. Phase formation analysis and lattice parameters

To understand the intermediate phase formation behaviour and reaction mechanism during synthesis of the ceramics, the powder was heated in the temperature range 800 ^{o}C to 1050 ^{o}C and each time, the calcined powder was analyzed by XRD. Fig. 3 shows the XRD patterns of BTN2 ceramics calcined at 800 and 1050^{o}C. Two intermediate phases $Bi_4Ti_3O_{12}$ and $BaTiO_3$ were observed in the specimen that was calcined at 800^{o}C (Fig. 3(a)).

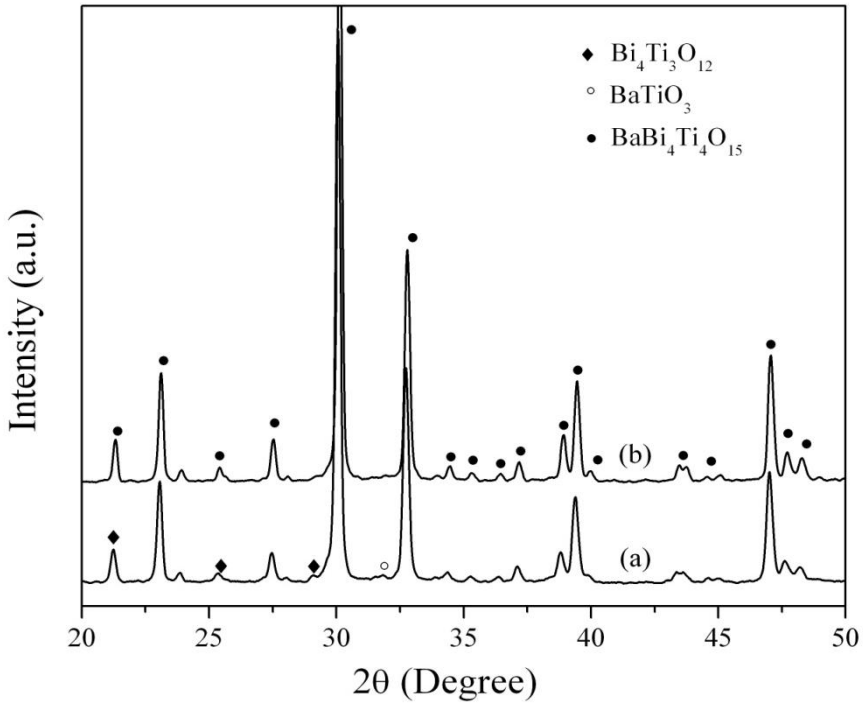

Fig.3. XRD pattern of BTN2 powder obtained after calcination at (a) 800^{o}C, and (b) 1050^{o}C for 4 h.

Finally, a pure phase of BBT was found in the specimen after calcination at 1050^{o}C for 4 hours as shown in Fig. 3(b). Hence, it can be concluded that the main mechanism of BBT formation is:

$$BaTiO_3 + Bi_4Ti_3O_{12} = BaBi_4Ti_4O_{15} \quad (1)$$

Similar mechanism was observed for all the other BTNX compositions. BTN6 specimen showed formation of $Na_2Ti_3O_7$ secondary phase along with main BBT phase. Fig. 4 shows

the phase formation sequences in BTN6 specimen. Fig 4(c) shows the presence of well crystallize $Na_2Ti_3O_7$ phase in 1050 ^oC calcined product.

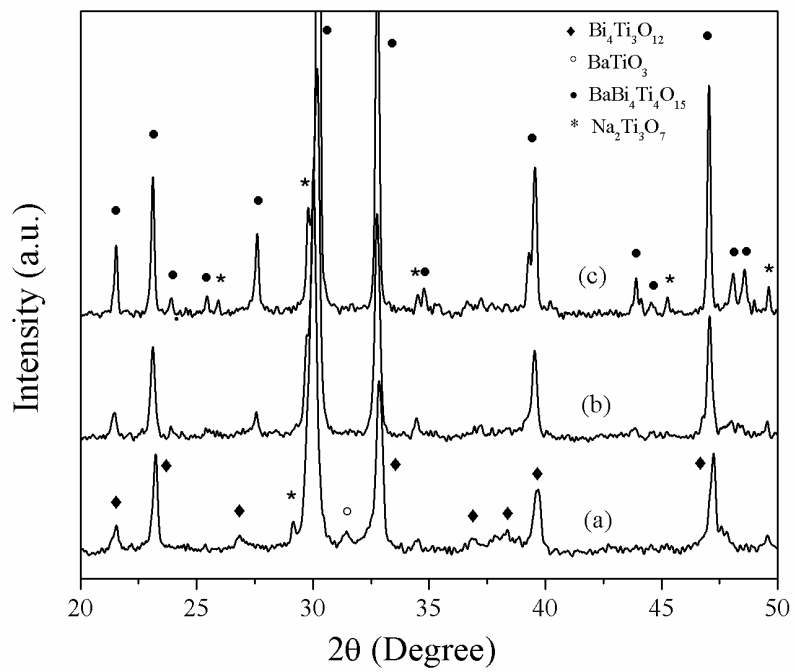

Fig.4. XRD pattern of BTN6 powder obtained after calcination at (a) 800^{o}C, (b) 900^{o}C, and (c) 1050^{o}C.

The effect of substitution on the change in lattice parameters of the ceramics was evaluated based on orthorhombic symmetry of the structure. The lattice parameters were calculated based on the relation:

$$\frac{1}{d^2} = \frac{h^2}{a^2} + \frac{k^2}{b^2} + \frac{l^2}{c^2} \qquad (2)$$

The lattice parameters, mainly *b* and *c* were found to decrease with increasing substitution rate as shown in Fig. 5. This decrease may be due to the replacement of Ba^{2+} by Na^{1+}, as the ionic radii of Na^{1+} is much smaller than Ba^{2+}. The ionic radii of Ti^{4+} and Nb^{5+} are almost similar and their substitution is unlikely to affect the lattice parameter.

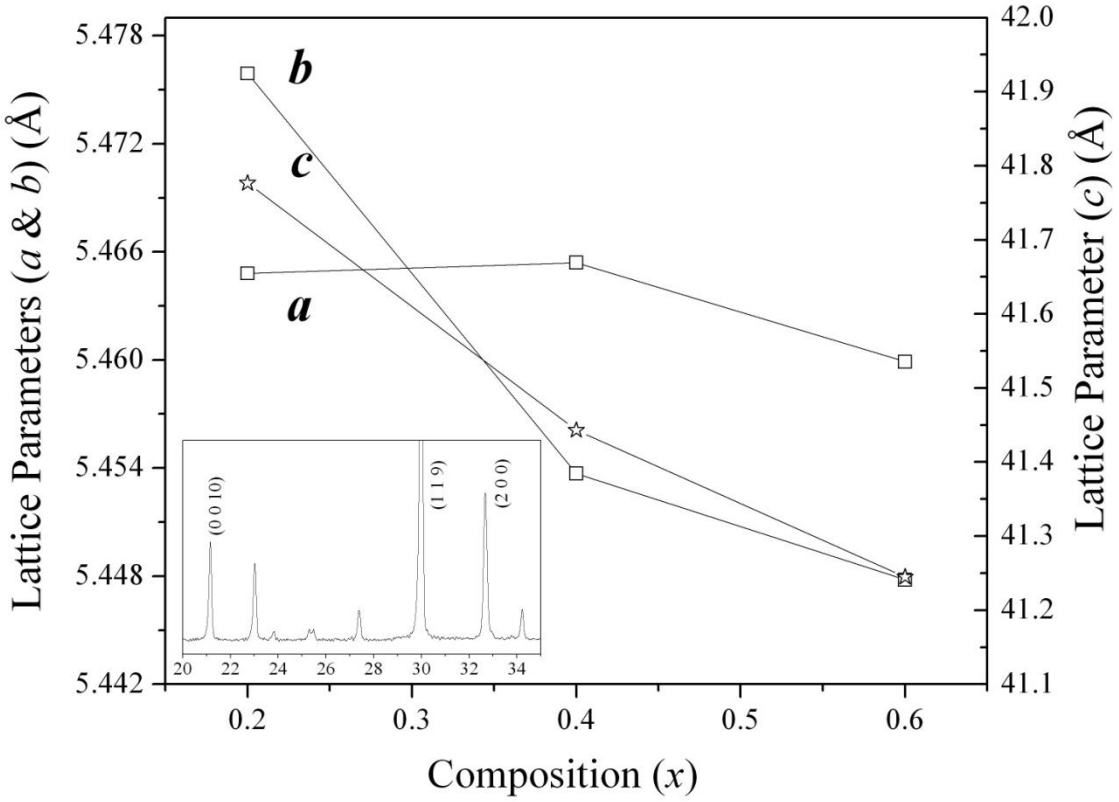

Fig.5. Lattice parameters with composition (x) for $Ba_{1-x}Na_xBi_4Ti_{4-x}Nb_xO_{15}$ ceramics. Inset XRD pattern shows the marked (*hkl*) peaks which were used to calculate lattice parameters.

5.2. Microstructure

Microstructure of as-sintered sample was obtained by SEM. Fig. 6 (a) and (c) shows the microstructure of BTN2 and BTN6 ceramics. It consists of plate like grains with random orientation of plate faces. It is known that plate like grain formation is a typical characteristic of bismuth layer-structured ferroelectrics as they have highly anisotropic crystal structure. The microstructure is dominated by the presence of large rounded edges platelet-like grains. The rounded edges are characteristic of liquid phase sintering. The grain size is found to increase with increase in substitution (Table 1). Due to the plate like structure the length increases with substitution. So, it may be concluded that Nb and Na accelerates the densification and grain growth in the ceramics.

Table 1 : Grain size (µm)of $Ba_{1-x}Na_xBi_4Ti_{4-x}Nb_xO_{15}$ for x = 0.2,0.4,0.6.

Formula	**BTN2**	**BTN4**	**BTN6**
Length	4.2	4.4	6.1
Breadth	2.5	3.1	4.8
Thickness	0.75	0.73	0.75

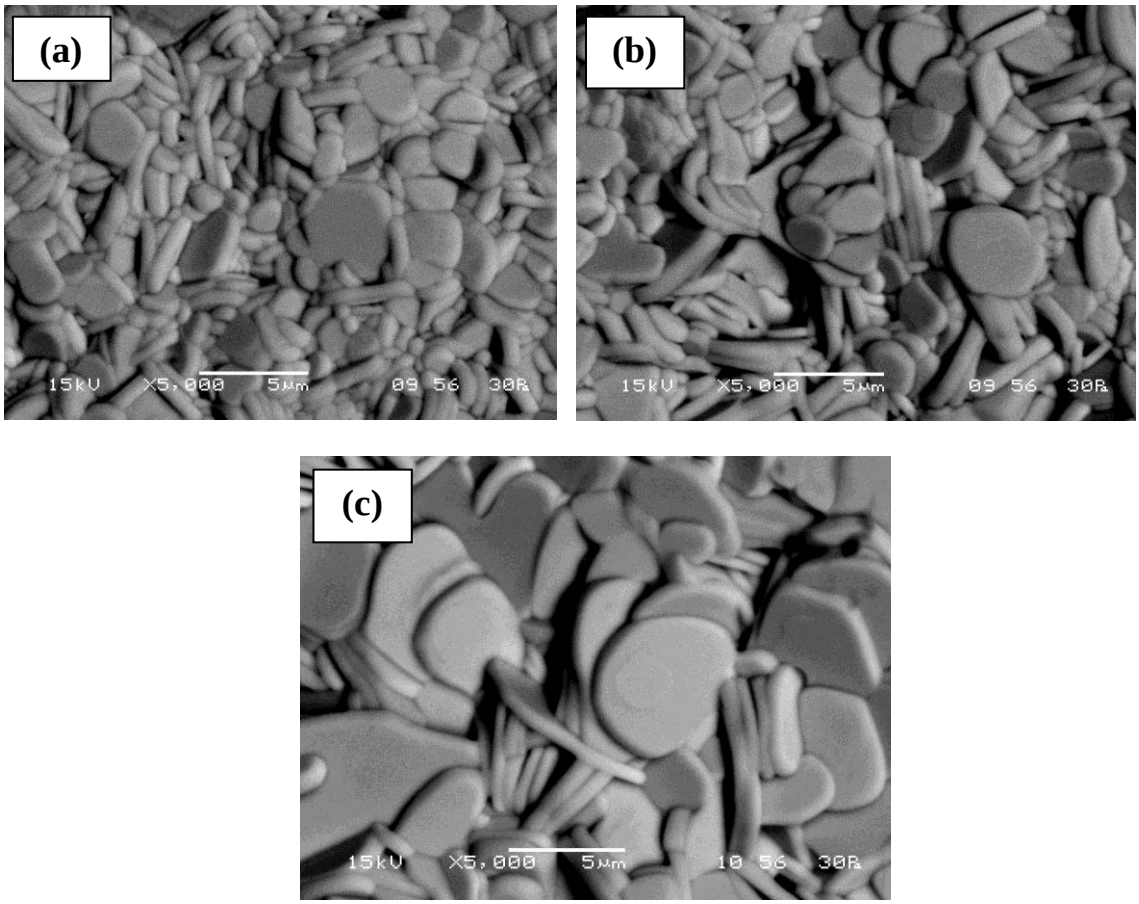

Fig.6. SEM Photographs of (a) BTN2, (b) BTN4, (c) BTN6.

5.3. Dielectric study:

Fig. 7 shows the temperature dependence of dielectric constant (ε') and dielectric loss (*tan* δ) of $Ba_{1-x}Na_xBi_4Ti_{4-x}Nb_xO_{15}$ ceramics measured at 100 kHz. The temperature of dielectric maximum (T_m) is found near ~400°C. The maximum dielectric constant (ε_m') increases for x = 0.2 compared to BBT. With further substitution it is found to decrease for $x \geq 0.4$ (Fig. 7(a)). This may be a result of the decrease in lattice parameter '*b'*, and associated 'A' type cation displacement. Smaller displacement leads to a decrease of polarization resulting in a reduction of dielectric constant. ε_m', T_m and room temperature dielectric constant (ε_{rm}) at 100 kHz are shown in Table 2. It can be noted that ε_{rm} increases with substitution for x = 0.2 which can be due to the slight shifting of ε_m' peak towards room temperature. Fig. 7(b) shows the *tan δ* vs temperature plots for the ceramics.

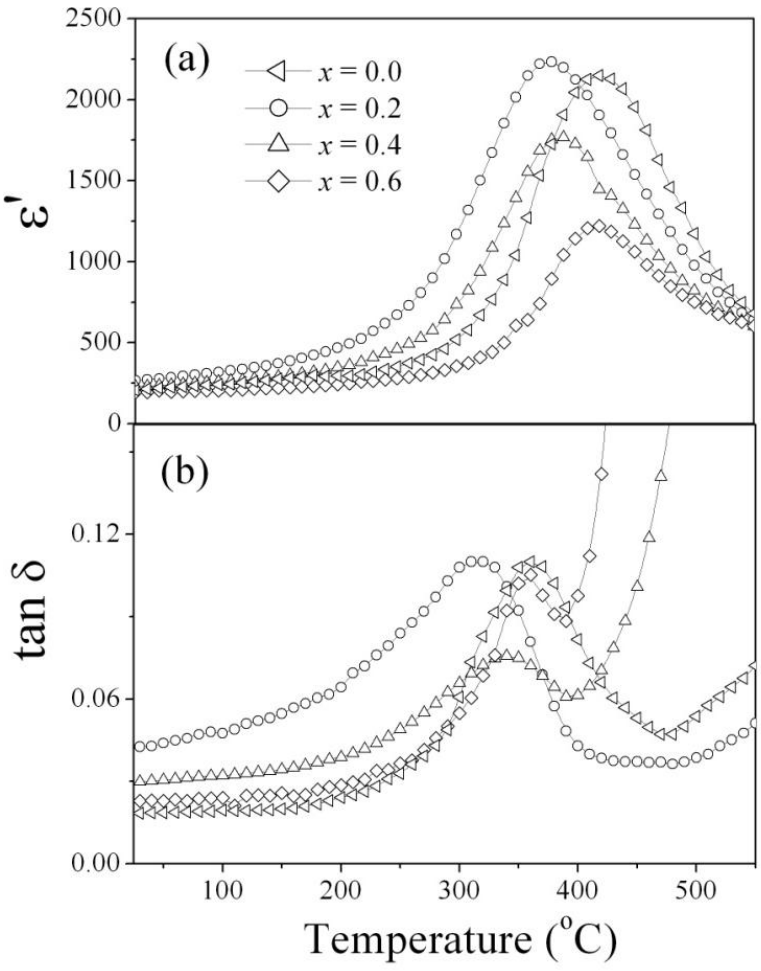

Fig.7. Temperature dependence of ε′ and *tan* δ for $Ba_{1-x}Na_xBi_4Ti_{4-x}Nb_xO_{15}$ ceramics at 100 kHz.

One of the important characteristics of a relaxor material is the frequency relaxation which is measured from the degree of relaxation parameter ΔT_m and is usually represented by:

$$\Delta T_m = T_{m(1\ kHz)} - T_{m(1\ MHz)} \quad (3)$$

The ΔT_m for x = 0.2 is in the range 15-20^{o}C. Fig. 8 shows that for x = 0.2 composition. However, the ΔT_m was found to be zero for compositions $x \geq 0.4$ (Fig. 9). This highlighted the fact that relaxor behavior was suppressed from x = 0.4 substitution.

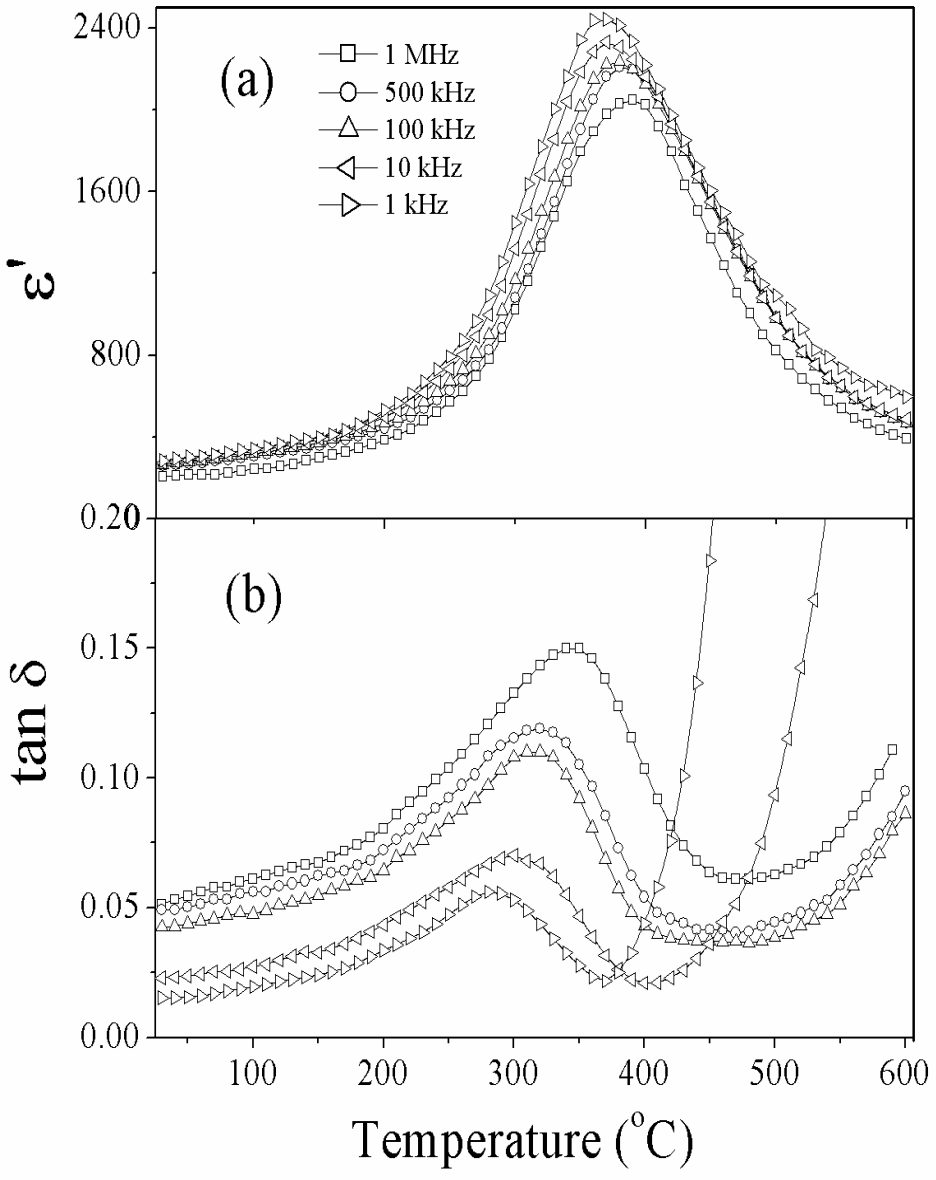

Fig.8. Temperature dependence of ε' and *tan* δ for $Ba_{1-x}Na_xBi_4Ti_{4-x}Nb_xO_{15}$ ceramics at various frequencies for x = 0.2.

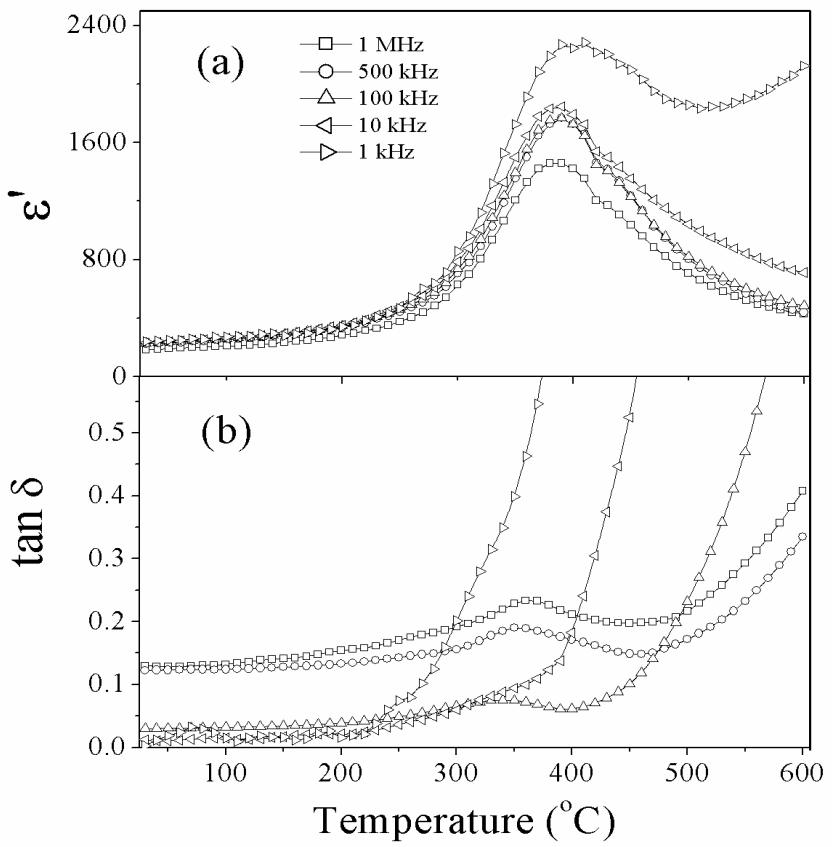

Fig.9. Temperature dependence of ε' and *tan* δ for $Ba_{1-x}Na_xBi_4Ti_{4-x}Nb_xO_{15}$ ceramics at various frequencies for $x = 0.4$.

Another important parameter; dielectric dispersion is frequently used for relaxor characterization. An empirical relation is proposed to describe the dielectric dispersion as

$$1/\varepsilon' - 1/\varepsilon_m' = (T - T_m)^{\gamma}/C_1 \qquad \text{----------(4)}$$

Where ε_m' is the maximum dielectric constant, γ and C_1 are constants. The values of γ lies in the range; $1 < \gamma < 2$. For an ideal ferroelectric to paraelectric phase transition $\gamma = 1$ and for ideal relaxors $\gamma = 2$. Fig. 10 shows the plot of log $(1/\varepsilon' - 1/\varepsilon_m')$ versus log $(T - T_m)$ for different compositions at 100 kHz and respective γ values. The γ values were found to decrease with increase in substitutions from 1.82 for BTN2 to 1.39 for BTN6. This may be due to the decrease in relaxor phenomena as stated above. The low γ value of BTN6 (1.39) suggests it a normal ferroelectrics. Structural studies of BBT reveal its relaxor effect is due to the structural disorder of Ba^{2+} and Bi^{3+} in the Bi_2O_2 layers [29]. In the present substitution,

Ba^{2+} is replaced by Na^{1+}. As a result, the structural disorder of the system decreases, thus suppressing the relaxor effect of the system.

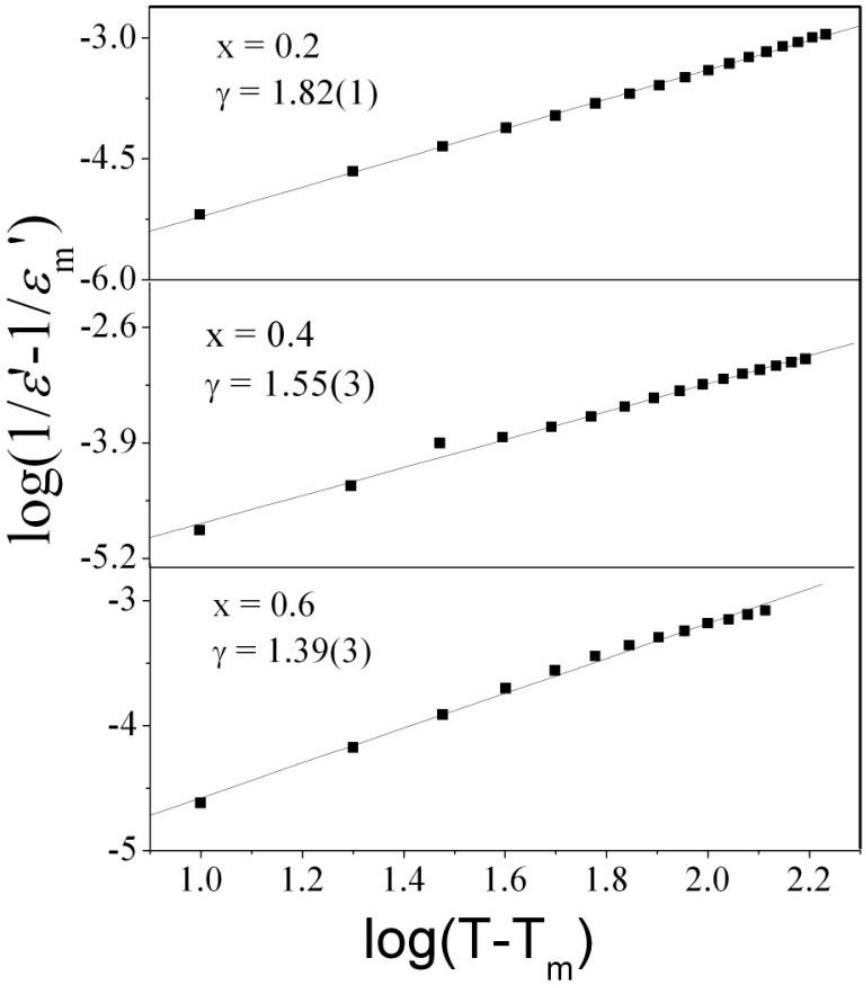

Fig.10. Plot of log $(1/\varepsilon' - 1/\varepsilon_m')$ versus log $(T - T_m)$ at 100 kHz for different $Ba_{1-x}Na_xBi_4Ti_{4-x}Nb_xO_{15}$ ceramics.

5.4. Ferroelectric Polarization versus Electric field study

The ferroelectric hysteresis loop of BTN*X* ceramics were obtained under a maximum applied electric field of 30 kV/cm. Fig. 13 shows the *P-E* loop for all the compositions recorded at room temperature and at a frequency of 100 Hz. With increase in substitution, the value of $2P_r$ increases for $x = 0.2$. Similar trend is also observed for $2E_c$ (Fig. 10). This behaviour of $2P_r$ and $2E_c$ is exactly similar to the change in the value of lattice parameter '*b*'. In this context it can be said that, '*b*' is the ferroelectric axis of the system.

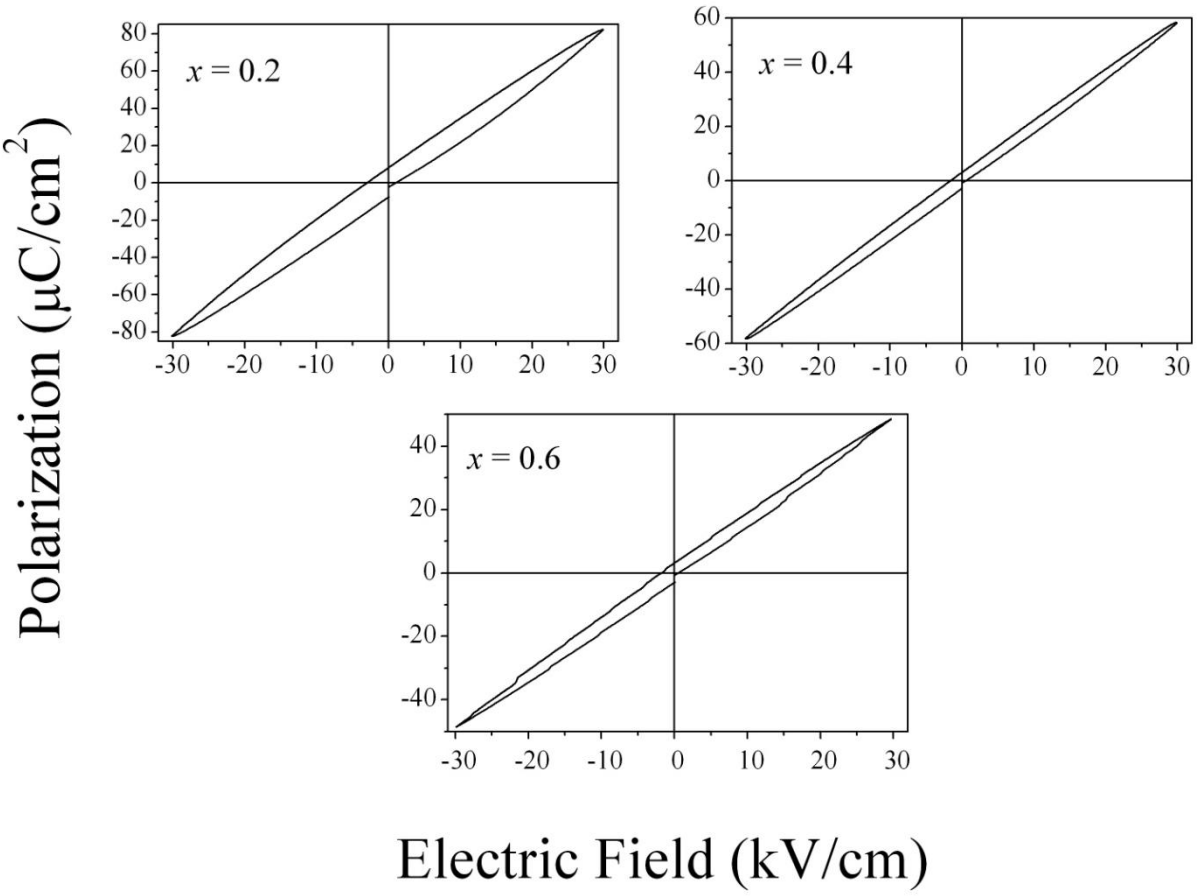

Fig.11. Plot of ferroelectric hysteresis loop measured at room temperature for different $Ba_{1-x}Na_xBi_4Ti_{4-x}Nb_xO_{15}$ ($x = 0.2, 0.4, 0.6$) ceramics.

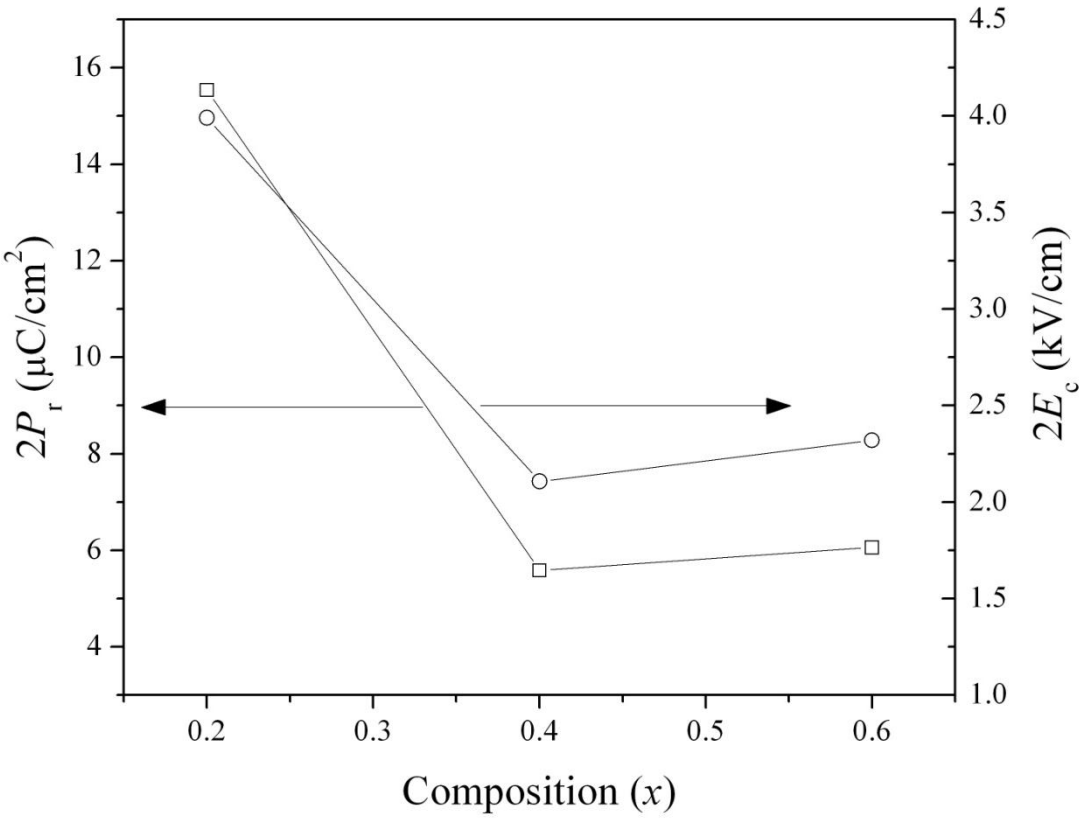

Fig.12. Plot of $2P_r$ and $2E_c$ measured at room temperature for different $Ba_{1-x}Na_xBi_4Ti_{4-x}Nb_xO_{15}$ (x = 0.2, 0.4, 0.6) ceramics.

5.5. DC conductivity

Impedance spectroscopy may shed a new light on the *dc* conductivity of BTN*X* ceramics. Cole-Cole plots obtained from impedance spectra are shown in Fig.13. It is observed that two different semicircles can be traced, which represent the grain and grain boundary regions, respectively. To calculate the resistance (R) and capacitance (C) values, an equivalent circuit is used to model the electrical response comprising of two parallel resistor-capacitor (RC) elements connected in series representing grain and grain-boundary regions. The values of R and C are determined from Cole-Cole plot.

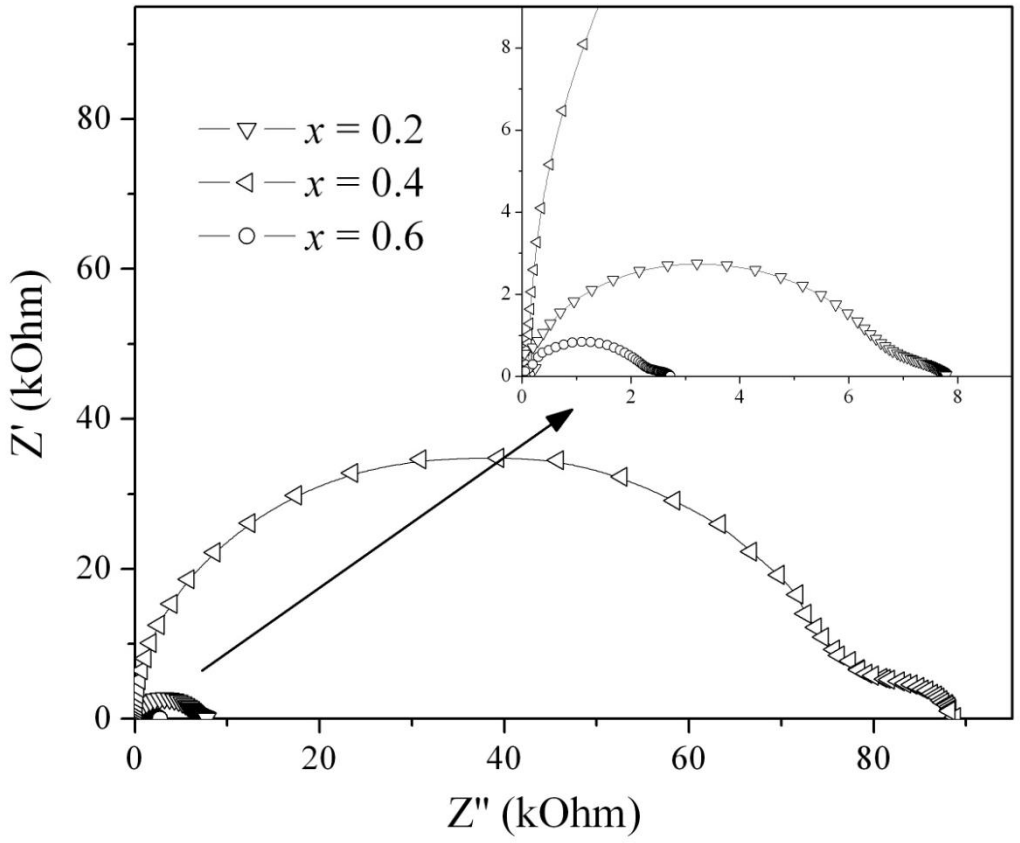

Fig.13. Cole-Cole plot for $Ba_{1-x}Na_xBi_4Ti_{4-x}Nb_xO_{15}$ (x = 0.2, 0.4, 0.6) ceramics at 600 ^oC.

The *dc* conductivities of grain and grain boundary regions are evaluated from the impedance spectra using the relation,

$$\sigma_{dc} = d/RA \quad (5)$$

where *d* is the thickness of the pellet, *A* is the electrode area and *R* is the grain or grain boundary resistance, which is derived by fitting the complex impedance data to the equivalent circuit model as described above. The values of *dc* conductivity at 600^{o}C for both grain and grain boundary are listed in Table 2. It can be noted that the *dc* conductivity is minimum for *x* = 0.2 composition.

Table 2: Room temperature permittivity (ε_{rm}), Maximum relative permittivity **(ε_m')** , maximum permittivity temperature (T_m) values at 100 kHz, dc conductivity for grain and grain boundary at 600 ^{o}C for different $Ba_{1-x}Na_xBi_4Ti_{4-x}Nb_xO_{15}$ ceramics.

Formula	**BTN2**	**BTN4**	**BTN6**
ε_{rm}	268	229	194
ε_m'	2234	1766	1219
T_m	380	390	420
σ_{dc} ($\Omega^{-1}cm^{-1}$) at 600 ^{o}C (grains)	1.40E-6	1.72E-5	4.66E-5
σ_{dc} ($\Omega^{-1}cm^{-1}$) at 600 ^{o}C (grain boundary)	4.57E-6	7.80E-5	1.34E-4

Chapter 6

Conclusions

6. Conclusions

In summary, Nb-substituted $Ba_{1-x}Na_xBi_4Ti_{4-x}Nb_xO_{15}$ ceramics was successfully synthesized by simple solid oxide reaction route. The substitution accelerates densification and grain growth in the ceramics due to low melting nature of Nb and Na. The relaxor behavior was suppressed from at x = 0.4 substitution due to the decrease in disorderness created by Ba in the structure. It can be said that, '*b*' is the ferroelectric axis of the system. The room temperature permittivity, remnant polarization are maximum and coercive field, the *dc* conductivity are minimum at $x = 0.2$ composition. This composition is highly promising for FRAM capacitor application and satisfies the requirement of FRAM.

Chapter 7

References

7. References:

[1] C.A.P. de Araujo, J.D. Cuchiaro, L.D. McMillan, M. Scott, J.F. Scott, Nature 374 (1995) 627.

[2] B.J. Kennedy, Y. Kubota, B.A. Hunter, Ismunandar, K. Kato, Solid State Commun. 126 (2003) 653.

[3] R.Z. Hou, X.M. Chen, Y.W. Zeng, J. Am. Ceram. Soc. 89 (2006) 2839.

[4] J. Tellier, Ph. Boullay, D.B. Jennet, D. Mercurio, J. Eur. Ceram. Soc. 27 (2007) 3687.

[5] A.V. Murugan, S.C. Navale, V. Ravi, Mater. Lett. 60 (2006) 1023.

[6] D. Xie, W. Pan, Mater. Lett. 57 (2003) 2970.

[7] T. Kimura, Y. Yoshida, J. Am. Ceram. Soc. 89 (2006) 869.

[8] H. Du, Y. Li, H. Li, X. Shi, C. Liu, Solid State Commun. 148 (2008) 357.

[9] C.-H. Lu, C.-Y. Wen, Mater. Lett. 38 (1999) 278.

[10] V. Shrivastava, A.K. Jha, R.G. Mendiratta, Solid State Commun. 133 (2005) 125.

[11] L.E. Cross, Ferroelectrics 151 (1994) 437.

[12] Gelfuso, M.V., Thomazini, D. and Eiras, J. A., J.Am.Ceram. Soc., 1999, 82, 92368-2372.

[13] Villegas, M., Caballero, A. C., Moure, C., Duran, P. and Fernandez, J. F,J. Am. Ceram. Soc., 1999, 82(9), 2411-2416.}

[14] B. Aurivillius, Arkiv. Kemi. 1 (54) (1950) 499–512.

[15] J. Tellier,Ph.Boullay,M.Manier,D.Mercurio, J. Solid State Chem. 177 (2004) 1829-1837.

[16] C. Miranda, M.E.V. Costa, M. Avdeev, A.L. Kholkin, J.L. Baptist, J. Eur. Ceram. Soc. 21 (2001) 1303–1306.

[17] G.C.C. da Costa, A.Z. Simoes, A. Ries, S.R. Foschini, M.A. Zaghete, J.A. Varela, Mater. Lett. 58 (2004) 1709–1714.

[18] A.J. Moulson, J.M. Herbert, Electroceramics, John Wiley & Sons Ltd., England, 2003.

[19] H. S. Shulman, M. Testorf, D. Damjanovic, and N. Setter, J. Am.Ceram. Soc., **79** [12] 3124–28 (1996).

[20] C. Voisard, D. Damjanovic, and N. Setter, J. Eur. Ceram. Soc., **19**[6–7] 1251–54 (1999).

[21] M. Villegas, A. C. Caballero, C. Moure, P.Duran, and J.F.Fernandez, J.Am.Ceram. Soc., **82** [9] 2411–16 (1999).

[22] I. Pribosˇic,D.Makovec, and M. Drofenik, J.Eur.Ceram.Soc.,**21** [10–11] 1327–31 (2001).

[23] Irena Pribosic, Darko Makovec, Miha Drofenik, J.Eur.Ceram.Soc., 21 (2001) 1327-1331.

[24] D.Benjannet,M.Elmaaoui& J.P.Mercurio, Journal of Electroceramics,11,101–106,2003

[25] SanjayR.Dhage, RenuPasricha, V.Ravi, Mater.Res.Bull.38 (2003) 1623.

[26] S.R.Dhage, S.P.Gaikwad, P.Muthukumar, V.Ravi, Mater.Lett.58 (2004) 2704.

[27] S.R.Dhage,Y.B.Khollam, S.B.Dhespand, H.S.Potdar, V.Ravi, Mate.Res.Bull. 39(2004)1993.

[28] M.Anilkumar, R.Pasricha, V.Ravi, Ceram.Inter.31(2005)889.

[29] Tellier, J., Boullay, Ph., Manier, M., and Mercurio, D., J. of Solid State Chem., 2004, **177**, 1829–1837.